# POLITECNICO DI TORINO
## Repository ISTITUZIONALE

Catalytic stability of a Ni-Catalyst towards biogas reforming in the presence of deactivating trace compounds

(Article begins on next page)

20 April 2024

# Accepted Manuscript

Catalytic Stability of a Ni-Catalyst Towards Biogas Reforming in the Presence of Deactivating Trace Compounds

Davide Papurello, Vitaliano Chiodo, Susanna Maisano, Andrea Lanzini, Massimo Santarelli

# 1 Catalytic stability of a Ni-catalyst towards biogas reforming in the presence of

# 2 deactivating trace compounds

3 Davide Papurello[b*], Vitaliano Chiodo[a], Susanna Maisano[a], Andrea Lanzini[b], Massimo Santarelli[b]

4 [a] *Institute CNR-ITAE "Nicola Giordano", Via S. Lucia sopra Contesse, 5 – 98126, Messina, Italy*

5 [b] *Department of Energy, Politecnico di Torino, Corso Duca degli Abruzzi 24, 10129, Torino – Italy*

6 *Corresponding author. Tel.:+393402351692. Email address: davide.papurello@polito.it

7

8 *Abstract*

9 Trace compounds contained in the produced biogas range from tens to thousands of ppm(v) and the gas

10 cleaning is crucial, as much as it is important the investigation of the trace compounds impact on the

11 reforming section and on the SOFC performance. The catalytic stability of a Ni-catalyst towards biogas

12 reforming in the presence of three types of deactivating compounds (sulfur, siloxanes and aromatic

13 compounds) was investigated. When the biogas is composed of a methane to carbon dioxide ratio >1 under

14 the tested operating conditions, the Ni catalyst stability is achieved. A $Ni/Al_2O_3$ catalyst appears suitable for

15 the steam reforming of biogas including contaminants, under the operative conditions adopted. On the

16 contrary, the effect of a biogas stream with composition $CH_4/CO_2=50/50$ vol. % is much more harmful under

17 steam reforming conditions both in terms of activity and stability. This result was due to $CO_2$-promoted

18 Boudouard reaction that leads to extensive carbon formation on the catalyst surface. Under this condition,

19 sulfur and D5 compounds in the biogas have a significant impact on the longevity of the Ni catalyst. Hence,

20 carbon formation rate is affected by the degree of catalyst poisoning due to adsorption and/or deposition of

21 other species on catalytic sites.

22 **Keywords:**

23 Catalytic stability, biogas, trace compounds, SOFC, Direct internal reforming

24

25 **Nomenclature:**

26 ASR, Area Specific Resistance;

27 CEM, Controlled Evaporator Mixer;

28 DIR, Direct Internal Reforming;

29 EIS, Electrochemical Impedance Spectroscopy;

30 FID, chromatography-Flame Ionization Detector;

31 FU, Fuel Utilization;

32      GC, Gas Chromatography;

33      GHSV, Gas Hourly Space Velocity;

34      LSCF, Lanthanum Strontium Cobalt Ferrite;

35      OFMSW, Organic Fraction Municipal Solid Waste;

36      ppb(v), parts per billion by volume;

37      ppm(v), parts per million by volume;

38      SEM, Scanning Electron Microscope;

39      SOFC, Solid Oxide Fuel Cell;

40      TAR, dark brown or black viscous liquid of hydrocarbons

41      TCD, gas chromatography-Thermal Conductivity Detector;

42      TEM, Transmission Electron Microscope;

43      TPB, Three Phase Boundary;

44      WWTp, Waste Water Treatment plant;

45      YSZ, Yttria-Stabilized Zirconia.

46

47

48

49

50

51

52

53

54

55

56

57

## 1. *Introduction*

Biogas coming from the anaerobic digestion of organic waste covers a crucial role regarding landfilling and pollutant reduction, matter recovery and energy production. Putrescible waste can derive from the domestic urban organic waste, agricultural waste, manure and sludge collected in wastewater treatment plants. Biogas consists of $CH_4$ (45-70 vol. %), $CO_2$ (30-50 vol. %), $N_2$ (<5 vol. %), $O_2$ (0-3 vol. %) and a wide variety of trace compounds. The type and quantity of trace compounds depend on waste treated [1–4]. In fact, trace compounds found in landfill biogas and from digestion of organic wastes are completely different [1,5]. Landfill gas quality is widely varying depending on the degradation status of the landfilled material as well as moisture and temperature condtions, all of which may vary considerably in different parts of the landfill body [5]. The higher amount of aromatic compounds found in landfill biogas compared to sewage or farm biogases is often associated with older waste even though elevated levels of aromatic compounds have also been measured in urban waste disposal bins [6–8]. The main trace compound contained in a biogas from the anaerobic digestion of organic wastes – both from WWTPs or municipal organic waste – is hydrogen sulfide ($H_2S$) [1,5,9]. The $H_2S$ concentration can range from 10 to thousands of ppm(v), and it is a function of the organic waste, digester temperature and pre-treatments process adopted to improve the methane yield [1,10]. Some pre-treatments can be adopted during the biogas production to reduce the sulfur content in the biogas, such as processes with metal oxides. Other processes are implemented outside the digester, mainly processes that adopt the physical adsorption solution to abate trace concentration [3,8,11–17]. Among energy generators, SOFCs are silent systems, with low emissions and high electrical and thermal efficiency. These systems can produce energy in a distributed way and they can be adopted in the next future to reduce the energy dependency from fossil fuels with high efficiency [8,18,19]. The cleaning process of biogas results to be mandatory in order to reduce the trace contaminants to achieve SOFC requirements [3,12,13,15,19–21]. A SOFC co-generator fed by biogas needs a reforming process to produce a more suitable gas mixture rich in hydrogen and carbon monoxide content, electrochemically suitable for the SOFC [22,23].

Biogas can be converted to synthesis gas either by dry reforming or by a combination of dry and steam reforming using appropriate catalysts [24–27]. Since the $CH_4$ to $CO_2$ (molar) ratio in biogas is about 1.5, dry reforming alone can lead to significant carbon deposition within the reactor [24,28,29]. Therefore, it is desirable to mix biogas with steam for reforming and generally, the $H_2O$ to $CH_4$ ratio (S/C) is maintained at 2 to avoid any coke formation [30,23,22]. Besides carbon deposition issues, the presence of impurities has a tremendous effect on the performance of the catalyst. Among these, the most studied contaminant for catalytic steam reforming is sulfur, in the form of $H_2S$, which leads to an almost total deactivation of the catalyst [31–33]. Catalyst poisoning occurs due to the strong adsorption of sulfur or other impurities on active sites, promoting by poisoning-metal electron affinity; this consequently, blocks or alters the adsorptivity of the other species [34,35]. Overall, the saturation coverage of sulfur and other species (silicon compounds) depends on the operating temperature, metal loading, and the partial pressure of reacting gasses.

94   Catalysts with lower metal loading lose activity at a faster rate compared to catalysts with higher metal
95   loading [36,37].

96   Moreover, the presence of higher molecular weight hydrocarbons ($C_nH_m$ such as ethane, propane, etc.)
97   and aromatic compounds (benzene, toluene, etc.) can significantly affect the formation of carbon species and
98   thus the effectiveness of the catalyst [38,39]. The formation of carbon on the catalyst under steam reforming
99   conditions may take place mostly through cracking of hydrocarbons and aromatic compounds as well as the
100  Boudouard reaction. In this way, researchers [40,41] determined the coking tendency for steam reforming of
101  methane in the presence of C2 and C3 hydrocarbons over a Ni catalyst, and an increasing of coking with
102  carbon number was noted especially in the presence of olefin species. D'Angeli et al. [42] have also shown
103  that coke formation increases with the molecular weight of the feed and that the deactivation rates during
104  steam-reforming of ethane and propane over Ni/MgO were higher compared to methane.

105  Although poisoning of Ni in the presence of $H_2S$ or hydrocarbons is well known, combined effects of
106  $H_2S$ with other contaminants – which are the typical case of biogas – are lacking in the literature. Hence, the
107  main objectives of our research are:

108  i)      to investigate the catalytic stability of a Ni-catalyst towards biogas reforming in the presence of
109          three types of deactivating compounds ($H_2S$, higher hydrocarbons, and siloxane compounds)
110          either alone or combined;

111  ii)     to analyze the catalytic performances when different biogas compositions are used;

112  iii)    to evaluate reforming options to increase catalyst lifetime and/or reduce the reformer operating
113          temperature;

114  iv)     to find the best performance regarding carbon deposition and voltage stability in an SOFC single
115          cell fed with a mixture that simulates the direct internal reforming of biogas;

116  v)      to investigate the SOFC performance fed by biogas with different trace compounds, starting
117          from sulfur compounds ($H_2S$) to continue with the addition of siloxanes (D4) and aromatic
118          compounds ($C_7H_8$).

119  The novelty of the paper, from the catalytic point of view, can be identified mainly on two aspects. The
120  first aspect is related to the combined effect of biogas contaminants on Ni catalytic stability; while the
121  second one is the performance evaluation of biogas contaminants depending on biogas stream composition in
122  terms of $CH_4/CO_2$ inlet ratio.

123

4

124 ## *2. Experimental*

125 ### *2.1. Catalytic experiments on the reformer Ni catalyst*

126   Catalytic experiments were carried out in a quartz fixed-bed reactor (i.d. = 4 mm; $h_{bed}$ = 2.0–4.0 cm) at

127 1073 K and atmospheric pressure. 0.2 g of commercial $Ni/Al_2O_3$ reforming catalyst [28,22,43]. The

128 operative temperature in the reactor was assured by three thermocouples located in different zones of the

129 catalytic bed. Before each test run, catalysts were reduced in-situ at T=1073 K for 1.5 h under hydrogen flow

130 (100 cc/min).

131   The flow rates of biogas ($CH_4+CO_2$) and poisoning species ($H_2S$, hydrocarbons, and siloxane) were

132 controlled by Brooks Instruments mass flow meters. In particular, the following poisoning concentrations

133 ranges were added in the reactant mixture: i) $H_2S$=0.4-1 ppm(v), ii) Decamethylcyclopentasiloxane (D5-

134 siloxane, $C_{10}H_{30}O_5Si_5$=0.5-1 ppm(v) and iii) hydrocarbons mixture=200-800 ppm(v)

135   Carbon formation during experiments was estimated by using a CHSN-O Carlo Erba elementary

136 analysis instrument, while A PHILIPS CM12 Transmission Electron Microscope (TEM) provided with a

137 high-resolution camera was used to analyze the morphology of both fresh and spent Ni catalysts. A field

138 emission Scanning Electron Microscope (SEM) equipped with EDAX microprobe (Philips XL30 S FEG)

139 was used to carry out qualitative and quantitative analysis of solid compounds (i.e., $SiO_2$) on the powders of

140 spent Ni catalysts.

141 ### *2.2. Electrochemical characterization of SOFC single cells*

142   Single SOFC cells were tested with simulated biogas to investigate the effects of direct internal

143 reforming and fuel contamination on the electrochemical performance of the fuel cell.

144   The laboratory test station is designed to test the planar SOFCs. A schematic diagram of the test rig is

145 provided in Figure 1. The test rig includes an oven, in which ceramic housings holding the planar cell are

146 placed. Moreover includes a gas mixing and distribution system; a humidification system, in which water is

147 added to dry gaseous streams; electric auxiliaries, which supply electricity to the oven and to the cell.

148 Finally, a data acquisition and control system is used to control the system.



149
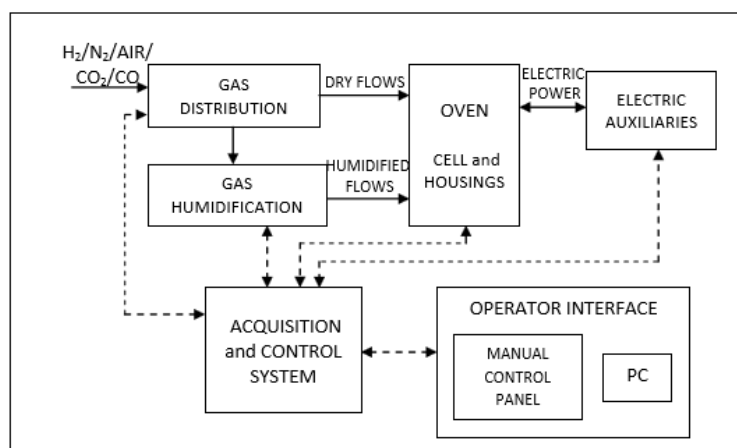
150 *Figure 1. Schematic diagram of the test-rig. Solid lines indicate mass and energy streams, while dashed lines*
151 *indicate data exchange between the acquisition and control system and the other subsystems.*

152     Two sintered alumina circular housings (diameter 80 mm) are located inside the oven. During
153 experiments, the tested cell is placed between the housings which provide gas distribution to both cell
154 electrodes and connect the cell to an external electronic load. The SOFC adopted in the tests is a planar
155 anode supported fuel cell. The cell is composed by a porous YSZ anode plus a support layer, a dense
156 electrolyte and a porous cathode made with LSCF. The cell has a circular section with an active surface of 47
157 $cm^2$ (it means a radius of about 3.86 cm) and the thicknesses of the different layers are reported in Table 1.
158 More detail on the experimental set-up can be found elsewhere [20,32,33,44].

159 *Table 1. Geometrical and material characteristics of the SOFC.*

| Layer | Material | Thickness |
|---|---|---|
| Anode (Support+ Active layers) | Ni/8YSZ | 517 μm |
| Electrolyte | YSZ | 5 μm |
| Cathode | LSCF | 45 μm |

160     The gas distribution system connects the test-rig to laboratory gas manifolds and ensures that dry gas
161 streams with specified flow rates and compositions are sent to the humidification system or directly to the
162 cell. This system is composed by pipes, valves (Swagelok), mass flow controllers (Bronkhorst) and a
163 Controlled Evaporator Mixer (CEM).

164

165 **3. Results**

166     **3.1. Boundary concentration of biogas poisoning on reformer section**
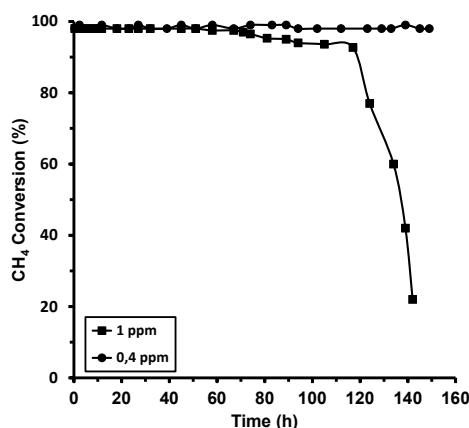
167         **3.1.1. $H_2S$ poisoning**

168     Sulfur is known as harmful species for Ni based catalysts and it's hardly to inhibit the catalyst poisoning
169 without specific experimental feedings [31,45]. Hence, the effect of $H_2S$ poisoning on the Ni catalyst
170 performance has been analyzed with respect to different concentrations (0.4 ppm(v) and 1 ppm(v)) in the
171 inlet gas stream. Previously, a catalytic steam reforming test was performed with a "clean" biogas stream in
172 order to verify the catalyst behavior in terms of carbon formation rate without poisoning.

173     Results in terms of methane conversion are shown for 0.4 and 1.0 ppm(v) of $H_2S$ concentration in the
174 fuel feed, respectively (Figure 2). The catalyst was stable for 150 hours of test with a GHSV of 15,000 $h^{-1}$
175 when $H_2S$ concentration was 0.4 ppm(v). In the experiment with 1 ppm(v) of $H_2S$, the Ni activity resulted in
176 a fast deactivation after about 60 hours of stable operation. The $CH_4$ conversion dropped down rapidly from
177 about 99% to 20%. This behavior would indicate that the breakthrough time is driven by sulfur concentration
178 in the reactant gas mixture. Furthermore, analysis performed on "used" Ni catalysts through a CHNS
179 analyzer, highlighted low rates of carbon formation ($\leq$0.1 mgC/$g_{cat}$·h) as well as on Ni catalysts working with
180 a clean biogas stream. This means that under the examined experimental conditions and 150 hours of time on

181 stream, the methane conversion rates are not affected by the poor carbon amounts deposited on catalyst
182 surfaces.

183



184
185 *Figure 2. Methane conversion vs time with $H_2S$ poisoning: $CH_4/CO_2$=60/40 mol%; H2O/CH4= 2 mol/mol;*
186 *GHSV=15,000 $h^{-1}$; T=1073 K; P=1 bar.*

### 3.1.2. Deactivation effects from heavier hydrocarbons

188 Generally, the reasons for deactivation of a Ni-based catalyst for the reforming of hydrocarbons are
189 primarily due to carbon deposition promoted by unsaturated compounds (i.e. olefins, aromatics, etc.). Thus,
190 effects of $C_2$ and $C_3$ species on Ni performances have been investigated through steam reforming
191 experiments performed in presence of different hydrocarbons concentrations the biogas stream.

192 Results showed a dramatically reduction of the methane conversion rate from about 99% to about 10%
193 after 50 h of time on stream in presence of an hydrocarbons concentration of 800 ppm(v) (calculated on
194 biogas stream under dry condition) (see Figure3), while a total concentration of $C_2$ and $C_3$ compounds of 200
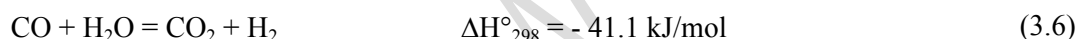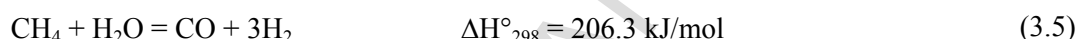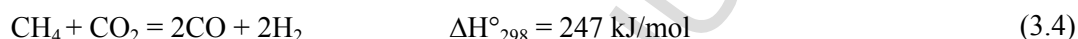195 ppm(v) would seem to have had no effect on the catalyst stability for 150 hours.
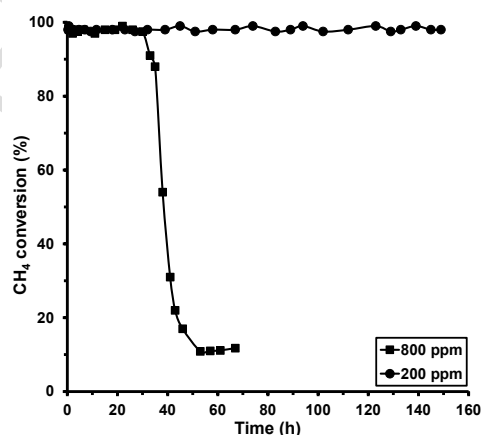


196
197 *Figure 3. Methane conversion vs time with higher hydrocarbons mixture addition: $CH_4/CO_2$=60/40 mol%;*
198 *$H_2O/CH_4$= 2 mol/mol; GHSV=15,000 $h^{-1}$; T=1073 K; P=1 bar.*

7

The different Ni catalyst behaviors shown in Figure 3, could be mainly explainable by equilibrium coking production (Eqs. 3.1,3.2 and 3.3).

$$C + H_2O = CO + H_2 \tag{3.1}$$

$$C_nH_{2n} = nC + nH_2 \tag{3.2}$$

$$2CO = C + CO_2 \tag{3.3}$$

In fact, the contribution of reaction 3.1, should increase with the increasing of heterogenous compounds to avoid massive coke deposition promoted by pyrolysis of species with carbon number >1 (Eq. 3.2) [39]. Nevertheless, an excessive presence of harmful species (i.e. alkenes) could exert a substantial effect on coke formation pathway [46]. In this context, it can be supposed that working with moderate poisoning concentrations ($\leq$200 ppm(v)) and under the conditions considered, an equilibrium among the main reactions of the process has been achieved (Eqs. 3.4-3.6).

$$CH_4 + CO_2 = 2CO + 2H_2 \qquad \Delta H°_{298} = 247 \text{ kJ/mol} \tag{3.4}$$

$$CH_4 + H_2O = CO + 3H_2 \qquad \Delta H°_{298} = 206.3 \text{ kJ/mol} \tag{3.5}$$

$$CO + H_2O = CO_2 + H_2 \qquad \Delta H°_{298} = -41.1 \text{ kJ/mol} \tag{3.6}$$

Data obtained by elementary analysis seem to confirm the above hypothesis; indeed a marked carbon formation (about 0.39 mgC/$g_{cat}$·h after 70 hours of test) was detected on spent Ni sample working with 800 ppm(v) of hydrocarbons poisoning (Table 2), while a minor carbon deposition (0.15 mgC/$g_{cat}$·h) was observed on Ni catalyst exposed to an hydrocarbons concentration of 200 ppm(v), as shown in Table 2.

*Table 2. Carbon and SiOx formation rates on spent Ni/Al$_2$O$_3$ catalysts: CH$_4$/CO$_2$=60/40 mol%; H$_2$O/CH$_4$= 2 mol/mol; GHSV=15,000 h$^{-1}$; T=1073 K; P=1 bar.*

|  | Hydrocarbons mixture* | | D5 Siloxane | |
|---|---|---|---|---|
| **Inlet gas concentration [ppm(v)]** | 800 | 200 | 1 | 0.5 |
| **Time on stream [h]** | 70 | 150 | 100 | 150 |
| **CH$_4$ conversion [mol%]** | 10 | 99 | 70 | 99 |
| **C formation rate [mgC/$g_{cat}$·h]** | 0.39 | 0.15 | $\leq$ 0.1 | $\leq$ 0.1 |
| **SiO$_2$ [wt%]** | - | - | 4.8 | 2.0 |

**\* Ethane, Ethylene, Acetylene, Propylene (200 ppm(v) for each)**

### 3.1.3. Siloxanes poisoning

Experiments were performed adding to the inlet gas stream different concentrations of decamethyl-cyclopenta-siloxane (D5) as the selected siloxane model compound. Results in terms of methane conversion

217 highlighted a decreasing of the Ni activity (from 99% to 70% after about 100 hours) when a concentration of
218 1 ppm(v) was added in the inlet gas stream. On the contrary, D5 concentration of 0.5 ppm(v) leaved
219 unchanged the methane conversion rate for 150 hours.

220     The Ni behavior can be attributed to its physical interaction with siloxanes compounds. In fact, D5
221 decomposes to $SiO_2$, which deposits on the catalyst surface compromising the catalytic activity (a similar
222 mechanism has been observed for the Ni-anode of the SOFC when exposed to D4 or D5 [47,48]). As
223 previously observed for spent Ni catalysts operated in presence of $H_2S$, the Ni samples exposed to different
224 D5 concentrations results minimally affected by carbon deposition (Table 2). While depositions of silicon
225 oxide were recorded on used Ni catalysts through SEM-EDAX analysis. As expected, the quantitative
226 analysis showed higher $SiO_2(s)$ formation on Ni samples operated with 1 ppm(v) of D5 ($SiO_2$ = 4.8 wt. %)
227 than samples exposed to 0.5 ppm(v) of D5 ($SiO_2$ = 2.0 wt.%). These results are in according with recently
228 studies carried out by authors that detected remarkable micro-silica deposits ($SiO_2$) on Ni spent catalyst
229 exposed to D5 effect under biogas steam reforming reaction [42].

230     *3.1.4. Co-poisoning effect*

231     In order to investigate on possible synergic effects of co-feeding of harmful compounds on the Ni
232 catalyst stability versus time, two kinds of poisoning were added simultaneously in the inlet gas stream
233 ('$H_2S$+Hydrocarbons mix' and 'Hydrocarbons mix+D5', respectively). Hence, maximum boundary
234 concentrations of each contaminant (0.4 ppm(v), 200 ppm(v) and 0.5 ppm(v) for $H_2S$, hydrocarbons and D5,
235 respectively) were mixed with the biogas stream.

236     Results given in Figure 4 show that the performances of the Ni catalyst did not suffer deactivation under
237 the simultaneous presence of two different kinds of poisoning species, at the concentrations examined
238 ($H_2S$=0.4 ppm(v)+Hydrocarbons=200 ppm(v) and Hydrocarbons=200 ppm(v)+D5=0.5 ppm(v)), when the
239 molar ratio $CH_4/CO_2$=60%/40% was used. The catalytic stability was recorded for about 150 hours for each
240 test; a methane conversion rate of about 99% was detected both in the presence of '$H_2S$+Hydrocarbons' and
241 'Hydrocarbons+D5' mixtures in the inlet gas stream.

242     Looking at the reformate gas compositions, the outlet molar fractions are very close to what is expected
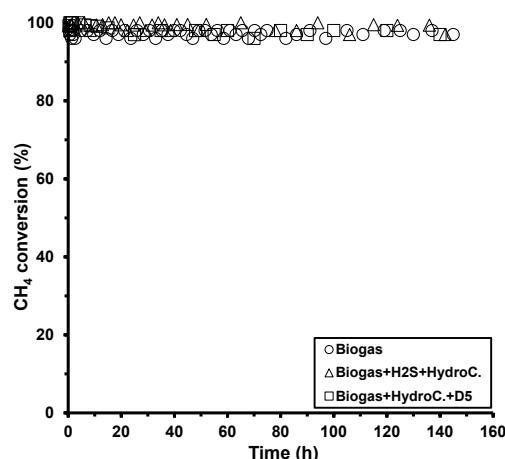243 from thermodynamic equilibrium, with an $H_2/CO$ molar ratio about 2.3 mol/mol (see Table 3).

244

*Figure 4. Methane conversion vs time: $CH_4/CO_2=60/40$ mol%; $H_2O/CH_4=2$ mol/mol; GHSV=15,000 $h^{-1}$;*
*T=1073 K; P=1 bar.*

*Table 3. Outlet stream composition: $CH_4/CO_2=60/40$mol%; $H_2O/CH_4=2$ mol/mol; GHSV=15,000 $h^{-1}$;*
*T=1073 K; P=1 bar.*

| Outlet stream | Thermodynamic Equilibrium | Experimental |
|---|---|---|
| | [Vol. %] | |
| $H_2$ | 49.8 | 48.3 |
| CO | 20.0 | 20.7 |
| $CO_2$ | 9.1 | 11.5 |
| $CH_4$ | 0.1 | 0.3 |
| $H_2O$ | 21.0 | 19.2 |

### 3.1.5. Impact of the inlet gas stream composition on biogas reforming

#### 3.1.5.1. Effect of carbon dioxide concentration

The influence of the $CH_4/CO_2$ ratio in the inlet gas stream on the Ni catalyst behavior was examined at 1073 K, $H_2O/CH_4=2$ mol/mol; 15,000 $h^{-1}$ of GHSV and atmospheric pressure. Experiments were repeated for 50/50 mol% $CH_4/CO_2$ working both without and with the presence of poisoning in the biogas stream. Stable catalytic performance (about 140 hours) was observed when using clean biogas. In the presence of impurities, deactivation occurred. By adding the hydrocarbons mixture in the feed gas the methane conversion dropped from 98% to 86% after ~80 hours of operation with stable performance; the loss of catalytic activity vs. time was more evident when either $H_2S$ or D5 were inserted in the inlet gas stream ($CH_4$ conversion dropped from 98% to about 30% after 70 and 90 hours for $H_2S$ and D5, respectively).

Finally, co-poisoning exposure under this 50/50 mol% $CH_4/CO_2$ mixture resulted in the worst condition in terms of catalyst stability with time. The two investigated combinations ($H_2S$+hydrocarbons and hydrocarbons+D5) resulted in a loss of Ni catalytic activity after only 20 hours of operation (see Figure 5). From the outlet stream composition, as reported in Table 4, an $H_2/CO$ molar ratio close to 2.1 mol/mol was obtained during the stable operation phase ($CH_4$ conversion rate=98%).

264
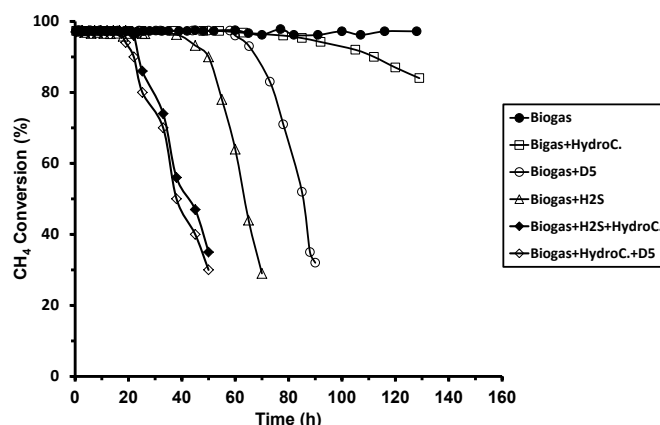265 *Figure 5. Methane conversion over time in the presence of different poisoning exposures:*
266 *$CH_4/CO_2=50/50mol\%$; $H_2O/CH_4=2$ mol/mol; GHSV=15,000 $h^{-1}$; T=1073 K; P= 1 bar.*

267

268 *Table 4. Outlet stream composition: $CH_4/CO_2=50/50mol\%$; $H_2O/CH_4=2$ mol/mol; GHSV=15,000 $h^{-1}$;*
269 *T=1073 K; P=1 bar.*

| Outlet stream | Experimental |
|---|---|
| | [Vol. %] |
| $H_2$ | 45.1 |
| CO | 21.4 |
| $CO_2$ | 12.8 |
| $CH_4$ | 0.4 |
| $H_2O$ | 20.3 |

270    The results from Figure 5, compared with the Ni catalyst performance reported in Figure 4, suggest that
271 a decrease of the $CH_4/CO_2$ molar ratio in the biogas stream strongly induces negative effects on the Ni
272 catalyst endurance. Moreover, the selectivity to $H_2$ production was reduced while the CO formation was
273 favored. This behavior is probably due to the reverse WGSR reaction ($CO_2+H_2=CO+H_2O$) promoted by
274 carbon dioxide absorption on Ni catalyst active sites [43,44]. However, this means that coke formation by
275 CO dissociation through the Boudouard reaction ($2CO=C+CO_2$) is favored, affecting in this way the catalyst
276 endurance. In addition, the Ni catalyst efficiency in a 50/50 vol% $CH_4/CO_2$ stream, compared to a 60/40
277 mixture, was more vulnerable to the presence of contaminants. Especially, the co-feeding cases were now
278 clearly more severe than the cases with only a single poison in the biogas stream.

279    **3.1.6. Catalyst post-test characterization**

280       **3.1.6.1.    Carbon formation rate**

281    Different samples of spent catalysts were analyzed by CHSN elementary analysis to better understand
282 the fundamental degradation mechanisms of catalytic steam reforming in the presence of impurities.

283    Results in Figure 6 show how the coke formation rate increased by increasing the carbon dioxide
284 concentration in the biogas composition. A deposition rate of about 0.41 $mgC/g_{cat}$·h was estimated for the
285 mixture $CH_4/CO_2=50/50$ vol% (under co-poisoning conditions). This observation seems to confirm that the

11

286 earlier hypothesis of competitive adsorption of carbon dioxide and $H_2O$ molecules on Ni active sites that

287 leave to carbon formation probably promoted by CO dissociation through the Boudouard reaction

288 (Eq.3.3).On the contrary, a biogas composition of $CH_4/CO_2=60/40$ vol% ensured stable catalyst performance

289 for about 150 hours at a GHSV of 15,000 $h^{-1}$, also under co-poisoning conditions.

290     According to literature [45,46], these results allow some considerations on the effect of sulfur and D5 on

291 carbon formation during the biogas steam reforming reaction. Indeed, experimental data indicate that the

292 carbon deposition rate can be accelerated by the presence of contaminants in the biogas stream: the

293 adsorption/precipitation of chemical poisoning species (e.g., sulfur and $SiO_2$) on the catalytic surface might

294 inhibit the carbon regasification with steam that protects the metallic phase from coke deposition.

295
296
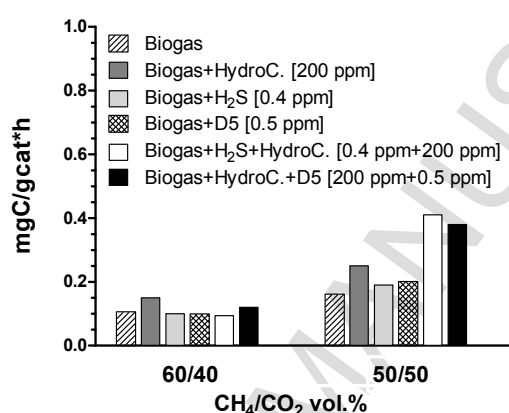


297
298     *Figure 6. Coke formation rate on spent samples catalyst: GHSV=15,000 $h^{-1}$; 1073K.*

299     ***3.1.6.2.    TEM and SEM microscopy evidences***

300     To evaluate carbon deposits, TEM micrographs have been taken on spent catalyst samples. TEM images

301 showed no evidence of large coke deposition when the feed gas was $CH_4/CO_2=60/40$ vol%. This result

302 agrees with the catalytic data previously reported, which showed only modest coke formation rates.

303



304
305
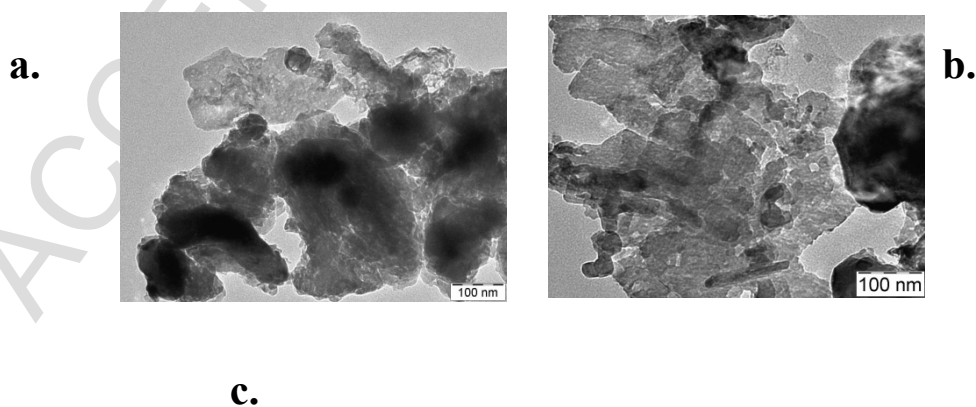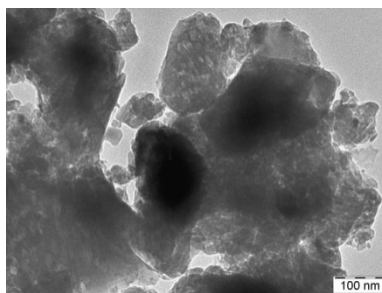
306
307  *Figure 7. TEM images on fresh and spent catalysts: a) Ni catalyst "fresh"; b) Ni catalyst "used"*
308  *$CH_4/CO_2$=60/40 mol%+$H_2S$+HydroC.; $H_2O/CH_4$=2 mol/mol; GHSV=15,000 $h^{-1}$; T=1073K; P=1bar; c) Ni*
309  *catalyst "used" $CH_4/CO_2$=60/40mol%+HydroC.+D5; $H_2O/CH_4$=2 mol/mol; GHSV=15,000 $h^{-1}$; T=1073 K;*
310  *P=1 bar.*

311      On the contrary, agglomerates of carbon depositions were observed on spent Ni catalysts working under

312  a biogas flow of $CH_4/CO_2$=50/50 vol%. As highlighted by TEM images (see Figure 8), graphitic carbon

313  deposits are present on the Ni surface. we suspect that the catalytic deactivation trends recorded during tests

314  with poisoning might be due to deactivation/degradation effects other than only carbon deposition (e.g.,

315  deposition/adsorption of foreign chemical compounds or atoms). Further evidence of this is presented in

316  section 3.

317
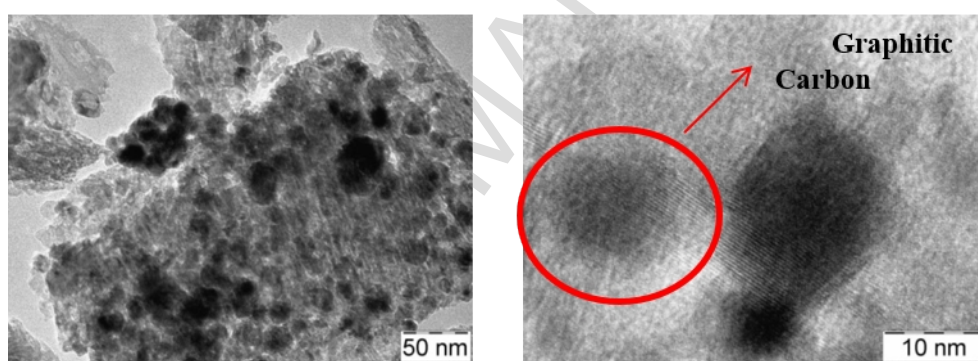


318
319  *Figure 8. TEM images on spent Ni catalyst at different magnifications: Ni catalyst "used"*
320  *$CH_4/CO_2$=50/50mol%+$H_2S$+HydroC.; $H_2O/CH_4$=2 mol/mol; GHSV=15,000 $h^{-1}$; T=1073 K; P=1 bar.*

321      SEM investigations were carried out in order to determine silicon oxide deposits on spent Ni catalyst

322  samples after exposure to D5 siloxane as a contaminant. As reported in Table 5, comparable concentrations

323  of $SiO_2$ were detected on catalyst samples used to reform biogas containing D5 in the inlet stream; however,

324  the durations of the experiments were not identical. The condition with biogas of $CH_4/CO_2$=50/50% was

325  more prone to deposit silica when normalized for the experiment duration.

326  *Table 5: SEM-EDAX analysis on spent Ni catalysts: T=1073 K, GHSV=15,000 $h^{-1}$.*

| SEM-EDAX | Operating Condition | | | |
|---|---|---|---|---|
| $SiO_2$ (wt. %) | $CH_4/CO_2$ (vol. %) | Hydrocarbon mix. (ppm(v)) | D5 (ppm(v)) | Time on stream (h) |
| 2.4 | 60/40 | 200 | 0.5 | 150 |
| 2.5 | 50/50 | 200 | 0.5 | 50 |

### 3.2. SOFC single cell testing

#### 3.2.1. Direct internal reforming study

The SOFC was fed by a gas mixture that simulates biogas fuel. The degree of direct internal reforming (DIR) of the biogas was varied from 0% (i.e., biogas is fully reformed externally before feeding the SOFC; in our experiments, we simulated directly the resulting reformate gas mixture) to 100% (in this case, the biogas is fully reformed inside the Ni-anode). Every experiment was carried out fixing the FU at 15% with a current density of 0.25 A/cm². The gas flow mixture of electrochemical fuel comes from the electrochemical hydrogen content, see the following table:

*Table 6. Biogas composition for different reforming degree.*

| DIR (%) | $H_2$ [mL/min] | $CH_4$ [mL/min] | CO [mL/min] | $CO_2$ [mL/min] | $H_2O$ [mL/min] | $\dot{V}_{tot}$ [mL/min] | $T_{bubble}$ [°C] |
|---|---|---|---|---|---|---|---|
| 0 | 346.2 | 6.6 | 184.8 | 40.9 | 58.7 | 637.1 | 49.6 |
| 25 | 220.3 | 54.9 | 117.6 | 59.8 | 88 | 540.6 | 64.2 |
| 50 | 127.5 | 90.5 | 68.1 | 73.75 | 109.6 | 469.5 | 75.3 |
| 75 | 56.4 | 117.8 | 30.1 | 84.85 | 126.2 | 414.9 | 87.4 |
| 100 | 0 | 139.4 | 0 | 92.9 | 139.4 | 371.7 | 93.5 |

In Figure 9, the voltage profile of the cell is given for the gas mixtures reported in Table 6. The cell voltage was quite stable during DIR 0, DIR 25 and DIR 50, while it oscillated at DIR 75. At DIR 100, technical limitations related to the maximum temperature achievable by the bubbler have reduced the voltage stability inducing the carbon deposition phenomena on the cell. At DIR 0%, an average voltage of 840 mV is attained, while at DIR 25 and at DIR 50, 850 mV and 860 mV are reached, respectively. The cell voltage increased up to DIR 50, which can be justified considering the calculated flows and the conditions that ideally should be present at the anode. Low $H_2O/H_2$ ratio allows to obtain a high-performance operation because reactants do not lower their partial pressure at the anode. At the same time a suitable $H_2O/CH_4$ ratio should be present because the reforming reactions take place.

14
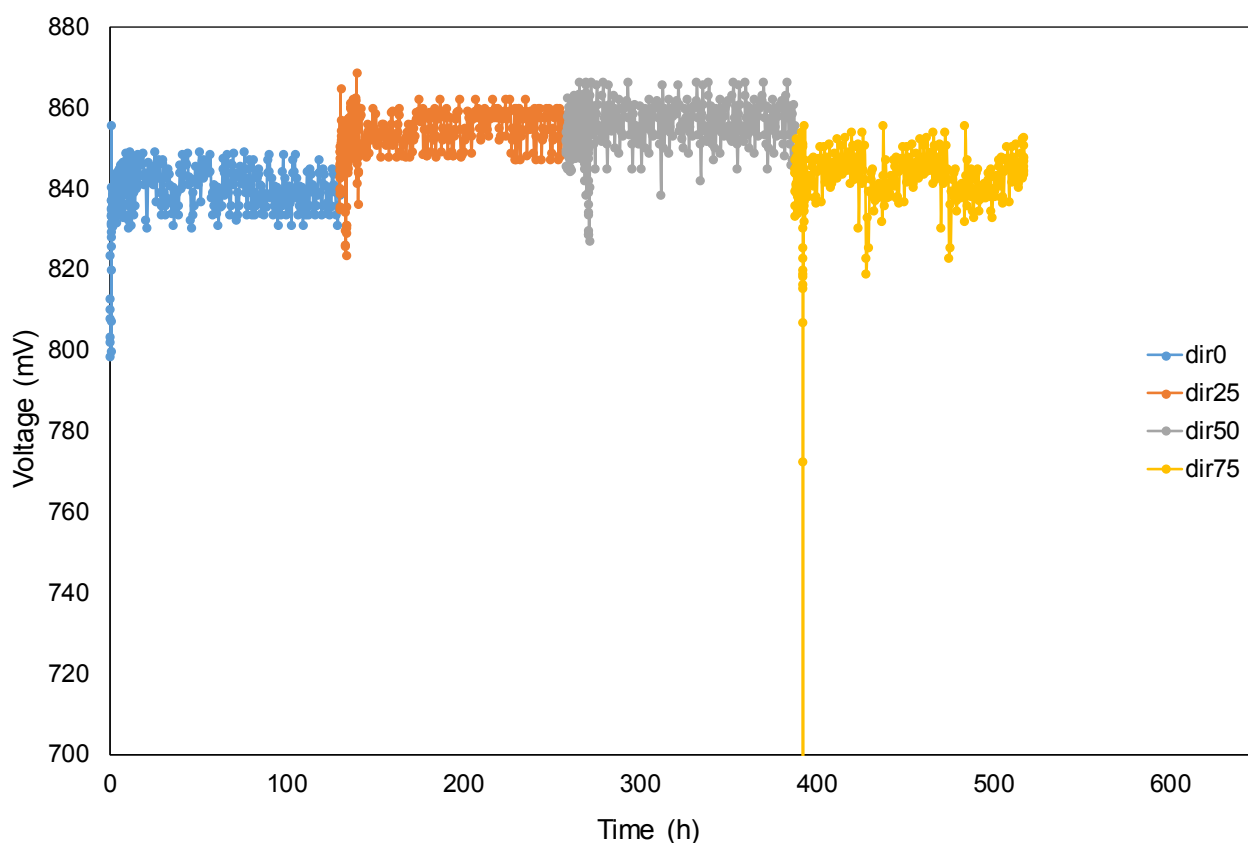
*Figure 9. Voltage profile at different DIR condition.*

The best biogas condition to feed the cell in terms of stable performance is closer to DIR 50 condition with a steam to methane and steam to hydrogen ratio comparable.

The Electrolyte Impedance Spectroscopy analyses are reported below. The cell monitoring has been done at the beginning and at the end of the time intervals every 12 h.

The results of the EIS analysis are shown in Figure 10 providing a comparison of the Nyquist diagrams obtained after 1 and 12 hours of operation in a given condition of DIR. The aim to reach in this phase is the determination of the optimal external reforming able to find a compromise between the cell performance and the economic impact.
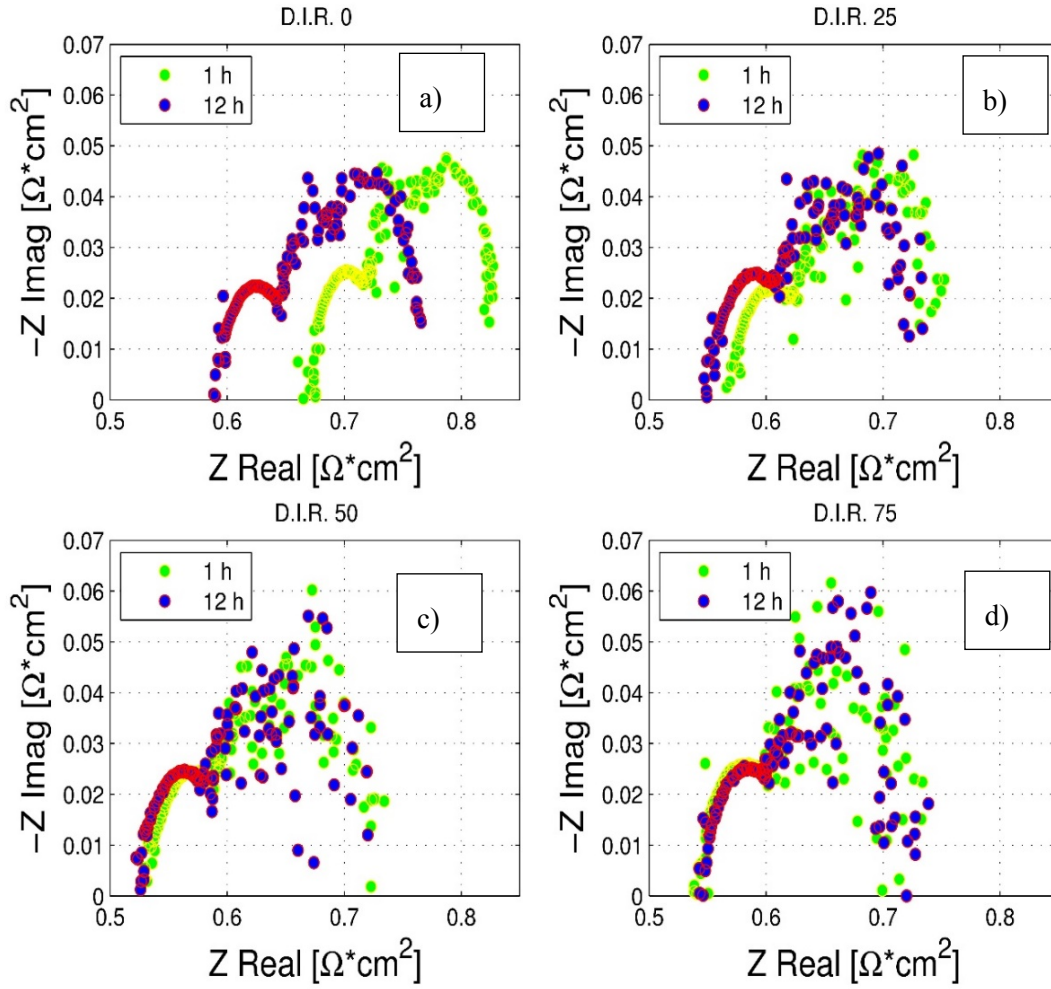
*Figure 10. EIS results for different DIR.*

Taking in consideration the electrochemical impedance spectroscopy analysis, the entity of the different losses can be extrapolated using the model reported elsewhere (see table 7) [20]:

*Table 7. Cell losses during operation.*

| DIR | Time (h) | $R_{ohm}$ $[\Omega \cdot cm^2]$ | $R_{el}$ $[\Omega \cdot cm^2]$ | $R_{tranp}$ $[\Omega \cdot cm^2]$ | $R_p$ $[\Omega \cdot cm^2]$ |
|---|---|---|---|---|---|
| **DIR0** | 1 h | 0.67 | 0.07 | 0.11 | 0.83 |
| **DIR0** | 12 h | 0.59 | 0.06 | 0.13 | 0.78 |
| **DIR 25** | 1 h | 0.56 | 0.07 | 0.11 | 0.72 |
| **DIR 25** | 12 h | 0.55 | 0.06 | 0.13 | 0.73 |
| **DIR 50** | 1 h | 0.53 | 0.05 | 0.14 | 0.72 |
| **DIR 50** | 12 h | 0.53 | 0.07 | 0.12 | 0.72 |

16

| | | | | | |
|---|---|---|---|---|---|
| **DIR 75** | 1 h | 0.55 | 0.05 | 0.1 | 0.7 |
| **DIR 75** | 12 h | 0.55 | 0.05 | 0.14 | 0.72 |

361      Observing the results reported above, the ohmic losses are not subjected to drastic variations in the 12 h

362      of observation for almost all the DIR analyzed. The only exception is represented by the DIR 0. However,

363      the main cause for the shift of the intersection with the real axis toward the left direction when the biogas

364      exposure time increases is a temperature variation at which the cell has been undergone when the reformate

365      biogas has been sent and this situation has increased the electrolyte conductivity.

366      The first arch of Nyquist plot, as previously discussed exemplifies the activation and the

367      electrochemical losses, which are stable in DIR 50 and DIR 75, while in the other two analyzed

368      configurations tend to decrease when the biogas's exposure time increases [15,47]. Finally, the low frequency

369      arch of Nyquist plot has tendency to increase its extension towards higher DIR because, being this arch

370      representative of the concentration losses, it has a higher impact where it is required to diffuse molecules

371      with higher dimensions. This situation happens when the gas mixture is over powered in methane and carbon

372      dioxide.

373      *3.2.2. Trace compounds single effect: sulfur compounds*

374      Considering an initial failure of the gas cleaning section ultra-low concentrations of $H_2S$ can reach the cell

375      during the operation. The possibility to not damage irreversibly the cell was proved from literature results

376      with a concentration of $H_2S$ below 1 ppm(v) [26,48,49]. The cell was tested at an operating temperature of

377      750 °C for 50% pre-reformed biogas with a steam-to-carbon ratio equal to 1. An ultra-low concentration of

378      $H_2S$ (0.46 ppm(v)) was sent to the anode of the cell. The test was carried out over 10 days and the EIS was

379      performed every 24 h. The ASR starts from 0.71 $\Omega cm^2$ after 24 h of test and every 24 h the ASR grew by an

380      average of 2 $\Omega cm^2$. The final ASR value reached was 0.98 $\Omega cm^2$.

381

382      An initial voltage drop followed by a steady state cell voltage was observed, as reported also in other

383      studies [32]. The degradation came about in the first 80 h of operation. In fact, the voltage assumes values

384      from 0.85 V to 0.74 V in the 240 h of test, but the fastest degradation was recorded in the first 80 h. The long

385      length of time required to achieve a stable condition is attributed to the low hydrogen sulphide concentration

386      that determines a longer interval time to cover the first layer of catalytic sites. Sulfur poisoning of the Ni-

387      anode is a phenomenon that is partially reversible. Once the $H_2S$ flow is stopped, a voltage increase that

388      suggests S desorption from Ni sites is observed. The desorption trends are quite similar to the corresponding

389      adsorption trends. As reported by Rasmussen and Hagen (2009), once the $H_2S$ concentration of 2 ppm(v) is

390      removed the cell performance is completely regenerated [48]. However, above 2 ppm(v) of $H_2S$, the

391      performance recovery is not complete. It is likely that some sulfur remains trapped in the three-phase

boundary (TPB), thus permanently increasing the anode polarization. This is supported by ASR value and EIS analysis. It can be seen that the $H_2S$ concentration in time leads to increases in the anode polarization due to concentration polarization, associated with the transport of gaseous fuel through the anode.
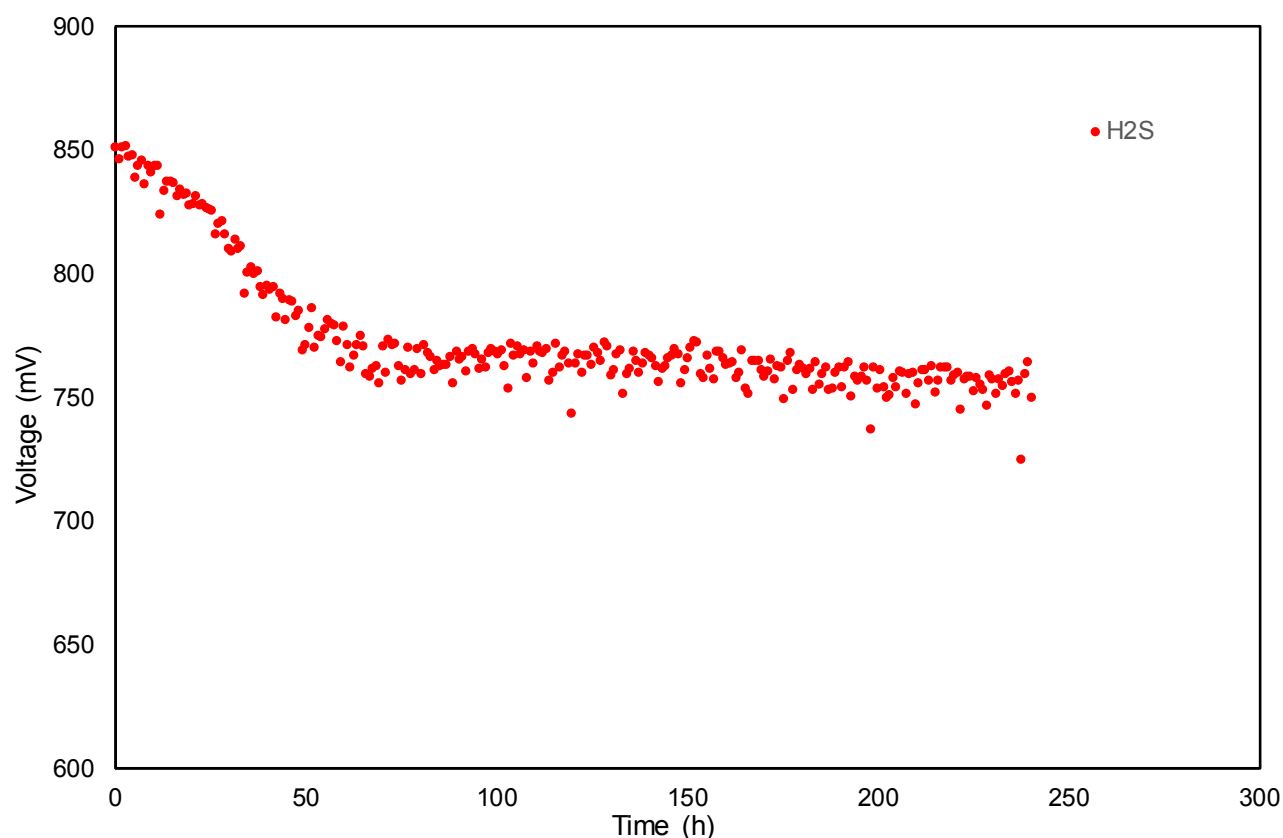


*Figure 11. Voltage trend at 10A during 10 days of test with $H_2S$.*

The stable condition is reached when the active surface achieves a high percentage of coverage. This situation determines a lower likelihood for the Sulphur to meet an active site. From this, a slowing in the coverage phenomenon is recorded. The main cause linked to the increase in the losses can be attributed overall to an increase in anodic over-potential respect to a variation of the ohmic effect. The main contribution is related to the low frequency term. This term is mainly affected by the presence of sulfur, this result is consistent with the results of other studies [50,51]. The frequency range of this arc is consistent with the range that can be expected for diffusion-related processes [52].

The presence of sulphur was found to have a greater effect on reforming reactions than electrochemical reactions, especially when compared to tests with hydrogen fuel on similar cells and condition [54]. This last statement allows us to consider the reforming reactions obstructed by the coverage caused by sulphur. Therefore, it is possible to deduce that the lack in reforming reactions leads to a high amount of no reacting methane that can take part in the cracking reaction. Consequence of the cracking is that the pores become blocked. This phenomenon manifests itself through an increase in the second arch of Nyquist plot. In fact,

18

410   the deposited carbon obstructs the entering of fresh fuel. However, the above mentioned is not the only

411   reading that can be given at low frequency arch.

412       Recent studies have shown that at SOFC operating temperature, also very small amounts of Sulphur (<1

413   ppm(v)) can interact with nickel at microstructural level. Prolonged exposure to fuel containing $H_2S$ at

414   elevated temperatures can lead to Ni coarsening due to adsorption [53]. The growth in Ni particles, results in

415   loss of percolation and determines the difficulty to spread fresh fuel.

416       The next figure shows that the voltage recovery is around 94% of the value before $H_2S$ administration

417   (Figure 12). The total voltage recovery is not fully respected because the degradation due to the previous

418   Sulphur presence was not totally reversible. This occurred both because the adsorbed sulphur is not totally

419   desorbed from the Ni-sites, as well as because the microstructural changings in Ni were not recovered.



420

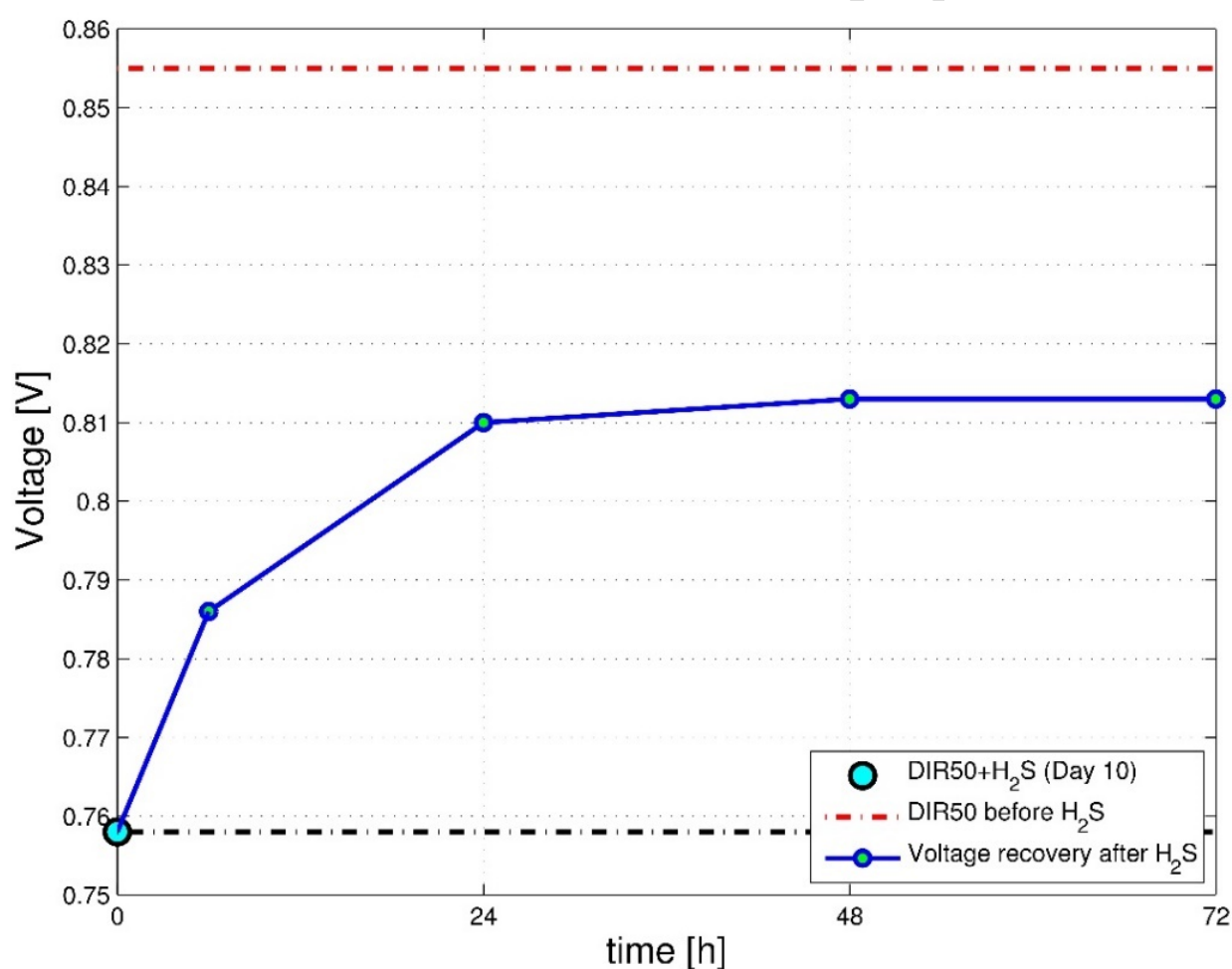421                          *Figure 12. Voltage trend after $H_2S$ removal.*

422         ***3.2.3. Trace compounds effect: multiple species impact***

423   The aim to test the single cell with biogas conditions closer to the reality other pollutants are added to the gas

424   mixture. These trace compounds are detect in biogas and reported in previous studies, such as siloxanes,

425   aromatic compounds and terpenes [1].

### *3.2.3.1. Double trace compounds impact on SOFC performance: sulfur and siloxane*

Few studies consider the impact of siloxane on SOFC performance but the combined effect with other pollutants are not reported [20,48]. Octamethylcyclotetrasiloxane (D4) was selected as model compound for siloxanes. Siloxanes were detected not only in biogas coming from WWTp, as reported in literature [54,55], but also in biogas coming from organic waste anaerobic digestion process [56]. D4 was detected in biogas coming from the dry anaerobic digestion of OFMSW with a range from 30 to 300 ppb(v). It is known that the more important siloxanes' effect is the formation of $SiO_2$. The tested siloxane is contained in certified bottles with 20 ppm(v) of D4 in pure $H_2$. The experiments were carried out considering a D4 concentration equal to 0.15 ppm(v) that acts in a period of 72 h. The EIS was carried out with intervals of 12 h and what emerged is shown in the following figure.
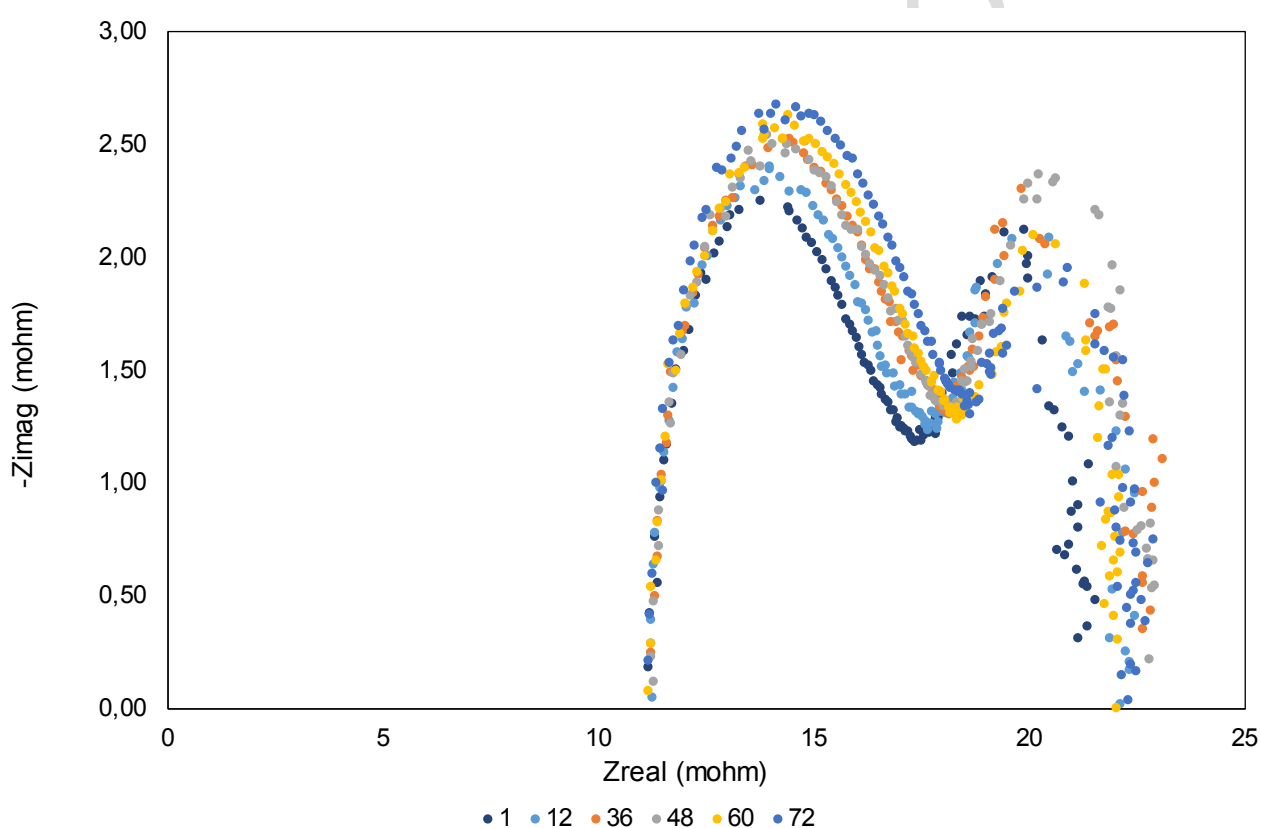


*Figure 13. EIS Nyquist diagram for $H_2S+D4$.*

*Table 8. Losses recorded in the EIS analysis using the electric circuit model approach.*

| Test condition | Time (h) | $R_{ohm}$ $[\Omega \cdot cm^2]$ | $R_{el}$ $[\Omega \cdot cm^2]$ | $R_{tranp}$ $[\Omega \cdot cm^2]$ | $R_p$ $[\Omega \cdot cm^2]$ |
|---|---|---|---|---|---|
| $H_2S$ (last) | 240 | 0.53 | 0.3 | 0.15 | 0.98 |
| $H_2S+D4$ | 1 | 0.53 | 0.3 | 0.16 | 0.99 |

20

| | | | | | |
|---|---|---|---|---|---|
| **H$_2$S+D4** | 72 | 0.53 | 0.36 | 0.21 | 1.08 |

439  After 1 h of exposure of the second pollutant, the polarization loss assumed a value similar to that
440  detected in the last test with the H$_2$S only. The situation appeared to be slightly different after 72 h, when the
441  increase in the total loss was about 0.09 $\Omega \cdot cm^2$ compared to the H$_2$S case. The losses were due to a 65% to
442  activation and to a 34% to transportation, determining an increase of 0.06 $\Omega \cdot cm^2$ and 0.05 $\Omega \cdot cm^2$ in the
443  high and low frequency arches, respectively. The total losses increased to 0.35 $\Omega \cdot cm^2$ compared to the clean
444  biogas, but 0.25 $\Omega \cdot cm^2$ were recorded when only H$_2$S acts. As other studies confirm [48], Si is able to
445  deposit and condense not only at the TPB, as happens with Sulphur, but deposits everywhere from the
446  distribution channel to the interface anode-electrolyte. However, after 72 h a condition of stability had still
447  not been reached because the D4 acted very slow (the rate is 0.04 V/50 h). Hence, slow but durable in time
448  degradation is attributed to silicon that can deposit it everywhere. This mechanism is deleterious from the
449  SOFC performance point of view; in fact the siloxanes act heavily on the cell decreasing as reported below.

450



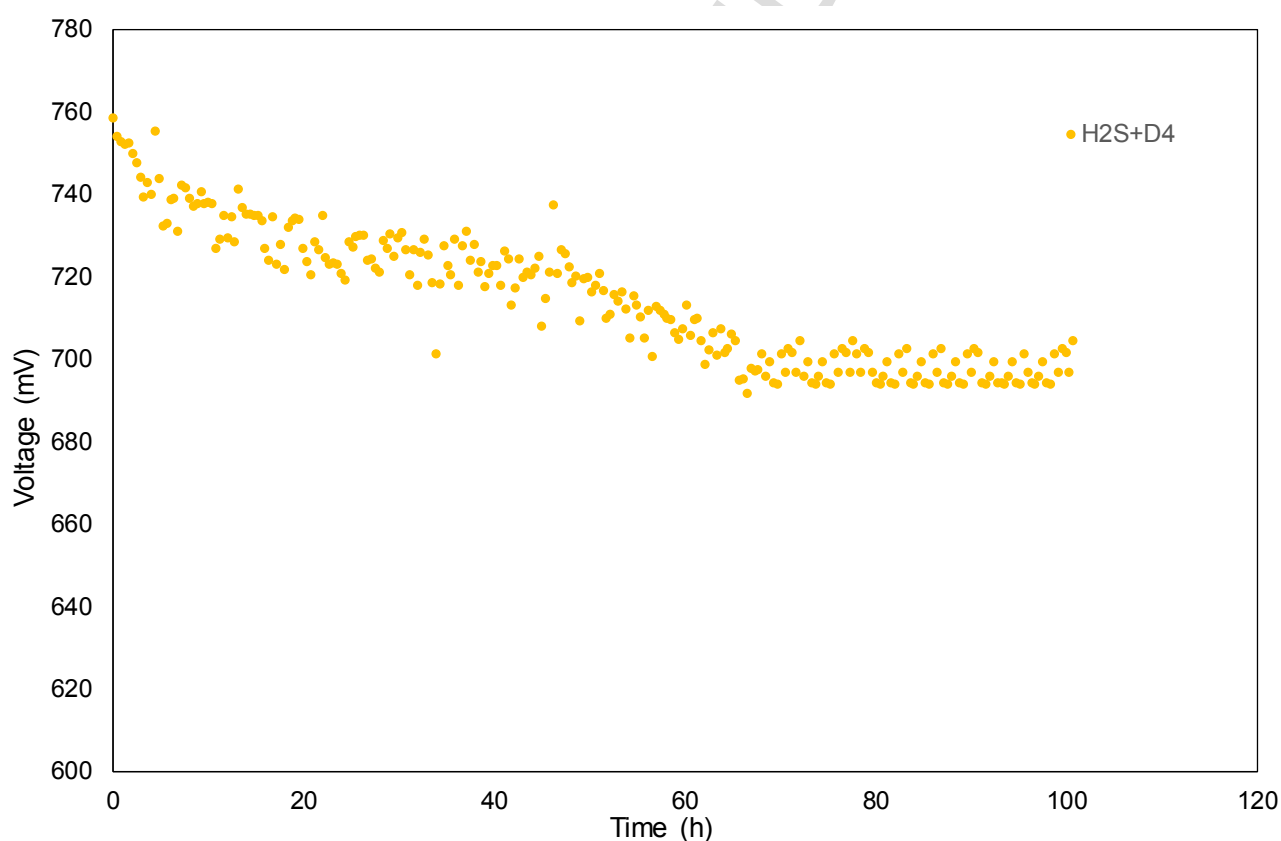451  *Figure 14. Voltage trend at 10A during 72 h of test with H$_2$S+D4.*

452  ### 3.2.3.2.  *Triple trace compounds impact on SOFC performance: sulfur, siloxane and*
453  *toluene*

454  Another trace compound was added to the gas mixture and cell performance are recorded and reported in
455  terms of EIS analysis and voltage profile along the test. The considered TAR was the toluene (C$_7$H$_8$). This is

456  one of the lightest TAR compounds and it can be easily detected in biogas from organic waste [1,5]. Toluene

457  is one of the TAR with the lower molecular weight thus highly reactive, for this reason, it represents the

458  worst condition for the cell operation.

459  The SOFC was fed with a concentration of toluene equal to 45.7 ppm(v). The tests were carried out over

460  six days, and the EIS was performed at intervals of 24 h each. As for the ohmic contribution, no variations

461  were recorded. However, the overall polarization tended to increase.

462  Losses increase of 0.15 $\Omega \cdot cm^2$ and mostly affect the low frequency arch of Nyquist plot. This last

463  aspect is verifiable observing that the high frequencies account only for 20% of the total. Considering all the

464  pollutants introduced, the $C_7H_8$ had the highest consequences on the diffusivity of fresh fuel at the anode.

465  Being the second arch related to the mass transport mechanisms, carbon deposition could have occurred.

466  This hypothesis is also confirmed by previous studies [20]. The presence of hydrocarbons in the biogas feed

467  could lead to the the cracking of molecules. This situation induces a decrease in the active sites that are

468  normally the promoter of reforming or electrochemical reactions. Under these conditions, methane is more

469  prone to take part in the cracking reaction compared to the reforming reactions. The carbon released by

470  cracking is deposited in the anode layer, so obstructing the inlet of fresh fuel.

471  The low-frequency arch, as already specified, is also affected by the $H_2S$ impact, even if this produces

472  consequences that are not alarming. In fact, the losses related to combined effect accounts for 0.15 $\Omega \cdot cm^2$ in

473  the most degraded condition, otherwise, the only $H_2S$ effect is of 0.02 $\Omega \cdot cm^2$. This means that, the losses

474  related to the $C_7H_8$ assume values around 0.12 $\Omega \cdot cm^2$. Considering Figure 15 the voltage profile shows the

475  cell performance decreasing when three different trace compounds are added to the SOFC cell. The

476  performance achieved are quite stable at the end, this demonstrates how the cell is not broken but it is

477  irreversibly affected by the trace compounds considered, when these compounds are removed from the gas
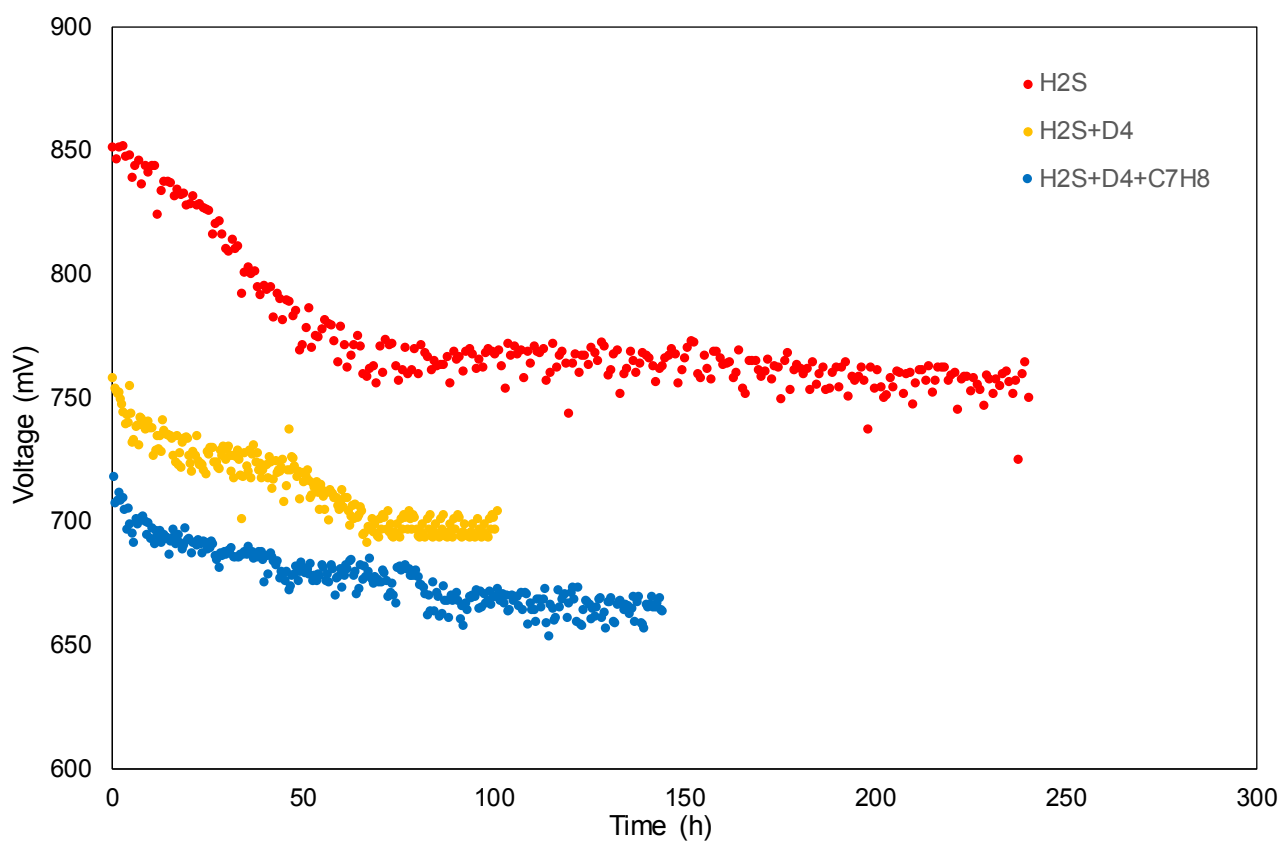
478  mixture, see Figure 16.

*Figure 15. Voltage trend at 10A during 6 days of test with $H_2S+D4+C_7H_8$.*

Figure 16 shows the iV curve made at the beginning of the test and after the removal of trace compounds, demonstrating that the SOFC performance are irreversibly affected.
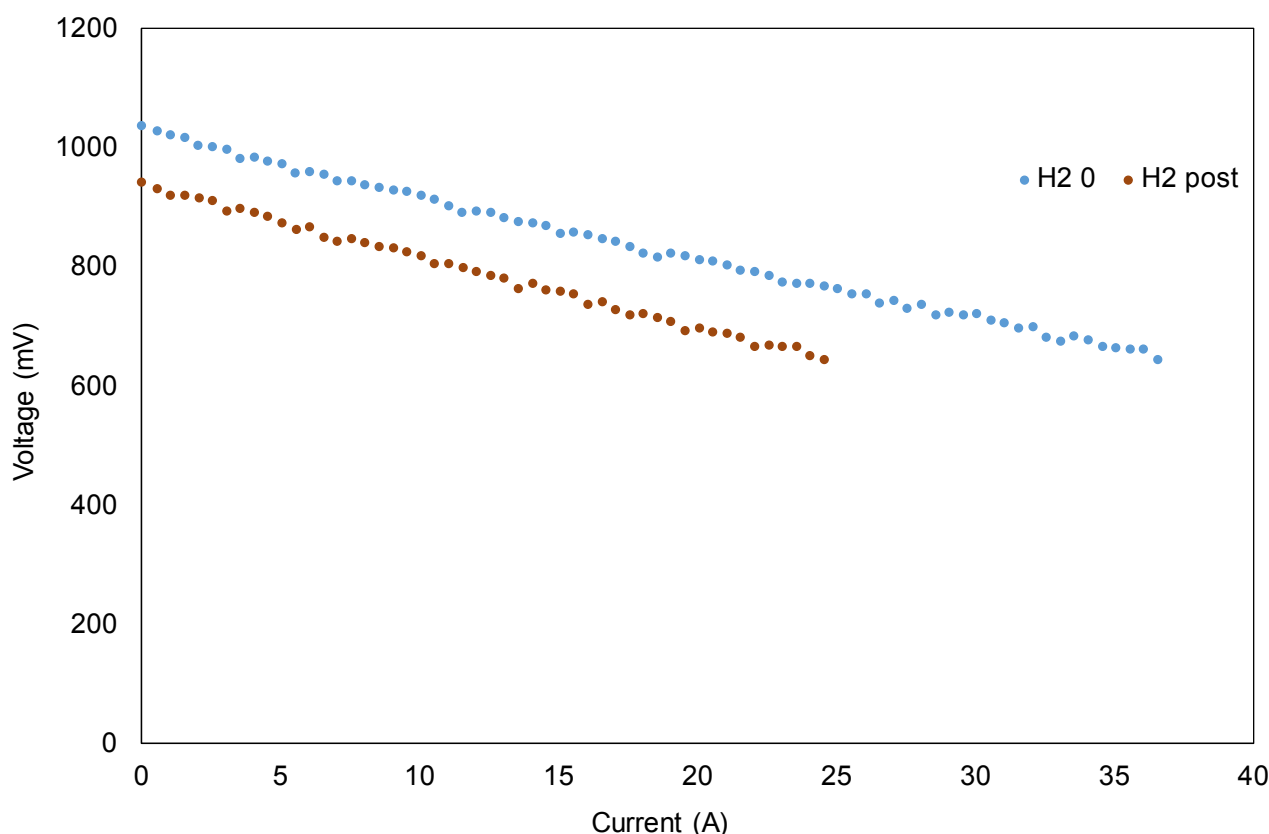
23

*Figure 16. iV curve in hydrogen made at the beginning and at the end of the test session.*

### 4. Conclusions

A Ni/Al$_2$O$_3$ catalyst appears suitable for the steam reforming of biogas including contaminants, under the operative conditions adopted (CH$_4$/CO$_2$=60/40 vol.%, T=1073 K, H$_2$O/CH$_4$=2 mol/mol and GHSV=15,000 h$^{-1}$). Some tolerance towards the presence of one or more poisoning compounds in the inlet gas stream has been shown (among H$_2$S≤0.4 ppm(v), C$_2$-C$_3$ hydrocarbons mixture ≤200 ppm(v), and D5≤0.5 ppm(v)). The combined effect of two poisoning compounds in the feed does not seem to affect the Ni catalyst stability (if the concentration of the contaminants are below a threshold limit) when the biogas is composed of a methane to carbon dioxide ratio >1 under the tested operating conditions.

On the contrary, the effect of a biogas stream with composition CH$_4$/CO$_2$=50/50 vol. % is much more harmful under steam reforming conditions both in terms of activity and stability, probably due mainly to the CO$_2$-promoted Boudouard reaction that leads to extensive carbon formation on the catalyst surface. Under this condition, sulfur and D5 compounds in the biogas have a significant impact on the longevity of the Ni catalyst. Hence, the carbon formation rate is affected by the degree of catalyst poisoning due to adsorption and/or deposition of other species (i.e. sulfur and/or silicon oxide) on catalytic sites.

The Ni-anode SOFC performance was investigated varying the DIR condition and testing the impact of trace compounds. DIR investigation proved that the single cell was able to withstand stable up to DIR 50. The best

24

502 performance was achieved in this condition given the low $H_2O/H_2$ ratio that allows to obtain a high-

503 performance operation because reactants do not lower their partial pressure at the anode. At the same time a

504 suitable $H_2O/CH_4$ ratio should be present because the reforming reactions take place. The combinations

505 from these conditions are well verified in the DIR50 condition.

506 Considering the trace compounds impact on SOFC performance, $H_2S$ single compound plus D4 and $C_7H_8$ as

507 model compounds for sulfurs, siloxanes, and aromatic compounds were investigated. Some conclusions are

508 resumed below, considering the EIS analysis:

509 • Ohmic losses: the presence of any species of contaminant in the feeding biogas does not damage the

510 electrolytic layer that preserves unchanged its conductive characteristics.

511 • Activation Losses: the drop in the activation losses is recorded to reach the highest value when the

512 $H_2S$ is sent to the anode, in fact, the increasing of the activation losses is of 0.26 $\Omega \cdot cm^2$. Even if $C_7H_8$ and

513 D4 have an influence on the performance, they produce an increase in losses equal to 0.03 $\Omega \cdot cm^2$ and 0.04

514 $\Omega \cdot cm^2$, respectively. The justification linked to these behaviours can be found on the effect that each

515 pollutant produces, i.e. the adsorption/desorption in the catalytic sites and the capability to deposit itself

516 everywhere in the cell structure, respectively.

517 • Transportation losses: the low frequency arch of the Nyquist plot is mostly affected by the presence

518 of $C_7H_8$, while the D4 concentration, below 150 ppb(v) and $H_2S$ do not influence most this loss. In fact, the

519 aromatic compound leads to an increase in the losses of about 0.12 $\Omega \cdot cm^2$ compared to the case when only

520 D4 and $H_2S$ act. This is mostly due to the carbon deposition that follows the reduced capacity of Ni sites to

521 promote reforming reactions.

522

526

527 **References**

528 [1] Papurello D, Soukoulis C, Schuhfried E, Cappellin L, Gasperi F, Silvestri S, et al. Monitoring of
529 volatile compound emissions during dry anaerobic digestion of the Organic Fraction of Municipal
530 Solid Waste by Proton Transfer Reaction Time-of-Flight Mass Spectrometry. Bioresour. Technol.,
531 vol. 126, 2012, p. 254–65.

532 [2] Papurello D, Silvestri S, Tomasi L, Belcari I, Biasioli F. Natural gas trace compounds analysis with
533 innovative systems : PTR-ToF-MS and FASTGC. Energy Procedia 2016;101:536–41.
534 doi:10.1016/j.egypro.2016.11.068.

535 [3] Papurello D, Schuhfried E, Lanzini A, Romano A, Cappellin L, Märk TD, et al. Proton transfer
536     reaction-mass spectrometry as a rapid inline tool for filter efficiency of activated charcoal in support
537     of the development of Solid Oxide Fuel Cells fueled with biogas. Fuel Process Technol 2015;130:78–
538     86. doi:10.1016/j.fuproc.2014.09.042.

539 [4] Papurello D, Lanzini A, Leone P, Santarelli M, Silvestri S. Biogas from the organic fraction of
540     municipal solid waste: Dealing with contaminants for a solid oxide fuel cell energy generator. Waste
541     Manag 2014;34:2047–56.

542 [5] Rasi S, Veijanen a., Rintala J. Trace compounds of biogas from different biogas production plants.
543     Energy 2007;32:1375–80. doi:10.1016/j.energy.2006.10.018.

544 [6] Statheropoulos M, Agapiou A, Pallis G. A study of volatile organic compounds evolved in urban
545     waste disposal bins. Atmos Environ 2005;39:4639–45. doi:10.1016/j.atmosenv.2005.04.013.

546 [7] Allen MR, Braithwaite A, Hills CC. Trace Organic Compounds in Landfill Gas at Seven U . K .
547     Waste Disposal Sites 1997;31:1054–61.

548 [8] Papurello D, Silvestri S, Tomasi L, Belcari I, Biasioli F, Santarelli M. Biowaste for SOFCs. Energy
549     Procedia 2016;101:424–31. doi:10.1016/j.egypro.2016.11.054.

550 [9] Rasi S, Läntelä J, Rintala J. Trace compounds affecting biogas energy utilisation - A review. Energy
551     Convers Manag 2011;52:3369–75. doi:10.1016/j.enconman.2011.07.005.

552 [10] Papurello D, Lanzini A, Schufried E, Santarelli M, Silvestri S. Proton Transfer Reaction-Mass
553     Spectrometry ( PTR-MS ) as a rapid online tool for biogas VOCs monitoring in support of the
554     development of Solid Oxide Fuel Cells ( SOFCs ). 6th Int PTR-MS Conf 2013;130:144–50.
555     doi:10.1016/j.fuproc.2014.09.042.

556 [11] Papurello D, Schuhfried E, Lanzini A, Romano A, Cappellin L, Märk TD, et al. Influence of co-
557     vapors on biogas filtration for fuel cells monitored with PTR-MS (Proton Transfer Reaction-Mass
558     Spectrometry). Fuel Process Technol 2014;118:133–40. doi:10.1016/j.fuproc.2013.08.011.

559 [12] Papurello D, Tomasi L, Silvestri S, Santarelli M. Evaluation of the Wheeler-Jonas parameters for
560     biogas trace compounds removal with activated carbons. Fuel Process Technol 2016;152:93–101.
561     doi:10.1016/j.fuproc.2016.06.006.

562 [13] Papurello D, Tognana L, Lanzini A, Smeacetto F, Santarelli M, Belcari I, et al. Proton transfer
563     reaction mass spectrometry technique for the monitoring of volatile sulfur compounds in a fuel cell
564     quality clean-up system. Fuel Process Technol 2015;130:136–46. doi:10.1016/j.fuproc.2014.09.041.

565 [14] Papurello D, Tomasi L, Silvestri S, Belcari I, Santarelli M, Smeacetto F, et al. Biogas trace compound
566     removal with ashes using proton transfer reaction time-of-flight mass spectrometry as innovative
567     detection tool. Fuel Process Technol 2016;145:62–75. doi:10.1016/j.fuproc.2016.01.028.

568 [15] Papurello D, Boschetti A, Silvestri S, Khomenko I. Real-time monitoring of removal of trace
569     compounds with PTR-MS: Biochar experimental investigation. Renew Energy 2018.
570     doi:10.1016/j.renene.2018.02.122.

571 [16] Nam S, Namkoong W, Kang J, Park J, Lee N. Adsorption characteristics of siloxanes in landfill gas
572     by the adsorption equilibrium test. Waste Manag 2013;33:2091–8.
573     doi:10.1016/j.wasman.2013.03.024.

574 [17] Lodewyckx P, Verhoeven L. Using the modified Wheeler-Jonas equation to describe the adsorption
575     of inorganic molecules: Chlorine. Carbon N Y 2003;41:1215–9. doi:10.1016/S0008-6223(03)00052-
576     6.

577 [18] Van Herle J, Membrez Y, Bucheli O. Biogas as a fuel source for SOFC co-generators. J Power

26

578       Sources 2004;127:300–12. doi:10.1016/j.jpowsour.2003.09.027.

579    [19]    Papurello D, Lanzini A, Tognana L, Silvestri S, Santarelli M. Waste to energy: Exploitation of biogas
580            from organic waste in a 500 Wel solid oxide fuel cell (SOFC) stack. Energy 2015;85:145–58.
581            doi:10.1016/j.energy.2015.03.093.

582    [20]    Papurello D, Lanzini A, Drago D, Leone P, Santarelli M. Limiting factors for planar solid oxide fuel
583            cells under different trace compound concentrations. Energy 2016;95:67–78.
584            doi:10.1016/j.energy.2015.11.070.

585    [21]    Chavez R-H, Guadarrama JJ, Kastner JR, Das KC, Buquoi Q, Melear ND. Biogas treatment by ashes
586            from incineration processes. Clean Technol Environ Policy 2003;37:2568–74. doi:10.1007/s10098-
587            015-0980-3.

588    [22]    Galvagno A, Chiodo V, Urbani F, Freni F. Biogas as hydrogen source for fuel cell applications. Int J
589            Hydrogen Energy 2013;38:3913–20. doi:10.1016/j.ijhydene.2013.01.083.

590    [23]    Chiodo V, Galvagno A, Lanzini A, Papurello D, Urbani F, Santarelli M, et al. Biogas reforming
591            process investigation for SOFC application. Energy Convers Manag 2015;98:252–8.
592            doi:10.1016/j.enconman.2015.03.113.

593    [24]    Effendi A, Zhang ZG, Hellgardt K, Honda K, Yoshida T. Steam reforming of a clean model biogas
594            over Ni/Al2O3 in fluidized- and fixed-bed reactors. Catal. Today, vol. 77, 2002, p. 181–9.
595            doi:10.1016/S0920-5861(02)00244-4.

596    [25]    Rostrup-Nielsen J, Bak Hansen J-H. CO2-Reforming of Methane over Transition Metals. J Catal
597            1993;144:38–49. doi:10.1006/jcat.1993.1312.

598    [26]    Izquierdo U, Barrio VL, Lago N, Requies J, Cambra JF, Gemez MB, et al. Biogas steam and
599            oxidative reforming processes for synthesis gas and hydrogen production in conventional and
600            microreactor reaction systems. Int. J. Hydrogen Energy, vol. 37, 2012, p. 13829–42.
601            doi:10.1016/j.ijhydene.2012.04.077.

602    [27]    Avraam DG, Halkides TI, Liguras DK, Bereketidou OA, Goula MA. An experimental and theoretical
603            approach for the biogas steam reforming reaction. Int. J. Hydrogen Energy, vol. 35, 2010, p. 9818–27.
604            doi:10.1016/j.ijhydene.2010.05.106.

605    [28]    Appari S, Janardhanan VM, Bauri R, Jayanti S. Deactivation and regeneration of Ni catalyst during
606            steam reforming of model biogas: An experimental investigation. Int J Hydrogen Energy
607            2014;39:297–304. doi:10.1016/j.ijhydene.2013.10.056.

608    [29]    Galvagno A, Chiodo V, Urbani F, Freni F. Biogas as hydrogen source for fuel cell applications. Int J
609            Hydrogen Energy 2013;38:3913–20. doi:10.1016/j.ijhydene.2013.01.083.

610    [30]    Chiodo V, Urbani F, Galvagno A, Mondello N, Freni S. Analysis of biogas reforming process for
611            molten carbonate fuel cells. J Power Sources 2012;206:215–21. doi:10.1016/j.jpowsour.2012.01.114.

612    [31]    Ashrafi M, Pfeifer C, Pröll T, Hofbauer H. Experimental study of model biogas catalytic steam
613            reforming: 2. Impact of sulfur on the deactivation and regeneration of Ni-based catalysts. Energy and
614            Fuels 2008;22:4190–5. doi:10.1021/ef8000828.

615    [32]    Papurello D, Lanzini A, Fiorilli S, Smeacetto F, Singh R, Santarelli M. Sulfur poisoning in Ni-anode
616            solid oxide fuel cells (SOFCs): Deactivation in single cells and a stack. Chem Eng J 2016;283:1224–
617            33. doi:10.1016/j.cej.2015.08.091.

618    [33]    Papurello D, Borchiellini R, Bareschino P, Chiodo V, Freni S, Lanzini A, et al. Performance of a
619            Solid Oxide Fuel Cell short-stack with biogas feeding. Appl Energy 2014;125:254–63.

620   [34]   Erekson EJ, Bartholomrw CH. Sulfur poisoning of nickel methanation catalysts. II. Effects of H2S
621           concentration, CO and H2O partial pressures and temperature on reactivation rates. Appl Catal
622           1983;5:323–36. doi:10.1016/0166-9834(83)80160-2.

623   [35]   Papurello D, Lanzini A, Drago D, Leone P, Santarelli M. Limiting factors for planar solid oxide fuel
624           cells under different trace compound concentrations. Energy 2016;95:67–78.
625           doi:10.1016/j.energy.2015.11.070.

626   [36]   Abild-Pedersen F, Lytken O, Engbæk J, Nielsen G, Chorkendorff I, Nørskov JK. Methane activation
627           on Ni(1 1 1): Effects of poisons and step defects. Surf Sci 2005;590:127–37.
628           doi:10.1016/j.susc.2005.05.057.

629   [37]   Sidjabat O, Trimm DL. Nickel-magnesia catalysts for the steam reforming of light hydrocarbons. Top
630           Catal 2000;11–12:279–82. doi:10.1023/A:1027212301077.

631   [38]   Hofmann P, Panopoulos KD, Fryda LE, Schweiger A, Ouweltjes JP, Karl J. Integrating biomass
632           gasification with solid oxide fuel cells: Effect of real product gas tars, fluctuations and particulates on
633           Ni-GDC anode. Int J Hydrogen Energy 2008;33:2834–44. doi:10.1016/j.ijhydene.2008.03.020.

634   [39]   Hofmann P, Panopoulos KD, Aravind P V., Siedlecki M, Schweiger A, Karl J, et al. Operation of
635           solid oxide fuel cell on biomass product gas with tar levels. Int J Hydrogen Energy 2009;34:9203–12.
636           doi:10.1016/j.ijhydene.2009.07.040.

637   [40]   Trimm DL. Catalyst design for reduced coking (review). Appl Catal 1983;5:263–90.
638           doi:10.1016/0166-9834(83)80156-0.

639   [41]   Sidjabat O, Trimm DL. Nickel-magnesia catalysts for the steam reforming of light hydrocarbons. Top
640           Catal 2000;11–12:279–82. doi:10.1023/A:1027212301077.

641   [42]   Angeli SD, Pilitsis FG, Lemonidou AA. Methane steam reforming at low temperature: Effect of light
642           alkanes' presence on coke formation. Catal Today 2015:119–28. doi:10.1016/j.cattod.2014.05.043.

643   [43]   Chiodo V, Urbani F, Galvagno A, Mondello N, Freni S. Analysis of biogas reforming process for
644           molten carbonate fuel cells. J Power Sources 2012;206:215–21. doi:10.1016/j.jpowsour.2012.01.114.

645   [44]   Papurello D, Lanzini A, Leone P, Santarelli M. The effect of heavy tars (toluene and naphthalene) on
646           the electrochemical performance of an anode-supported SOFC running on bio-syngas. Renew Energy
647           2016;99:747–53. doi:10.1016/j.renene.2016.07.029.

648   [45]   Abild-Pedersen F, Lytken O, Engbæk J, Nielsen G, Chorkendorff I, Nørskov JK. Methane activation
649           on Ni(1 1 1): Effects of poisons and step defects. Surf Sci 2005;590:127–37.
650           doi:10.1016/j.susc.2005.05.057.

651   [46]   Didenko LP, Savchenko VI, Arutyunov VS, Sementsova LA. Steam reforming of methane mixtures
652           with ethylene over an industrial nickel catalyst. Pet Chem 2008;48:22–7. doi:10.1007/s11494-008-
653           1004-x.

654   [47]   Haga K, Adachi S, Shiratori Y, Itoh K, Sasaki K. Poisoning of SOFC anodes by various fuel
655           impurities. Solid State Ionics 2008;179:1427–31. doi:10.1016/j.ssi.2008.02.062.

656   [48]   Madi H, Lanzini A, Diethelm S, Papurello D, Van herle J, Lualdi M, et al. Solid oxide fuel cell anode
657           degradation by the effect of siloxanes. J Power Sources 2015;279:460–71.
658           doi:10.1016/j.jpowsour.2015.01.053.

659   [49]   Choudhary V., Uphade B., Mamman A. Simultaneous steam and CO2 reforming of methane to
660           syngas over NiO/MgO/SA-5205 in presence and absence of oxygen. Appl Catal A Gen 1998;168:33–
661           46. doi:10.1016/S0926-860X(97)00331-1.

662    [50]    Avraam DG, Halkides TI, Liguras DK, Bereketidou OA, Goula MA. An experimental and theoretical
663           approach for the biogas steam reforming reaction. Int. J. Hydrogen Energy, vol. 35, 2010, p. 9818–27.
664           doi:10.1016/j.ijhydene.2010.05.106.

665    [51]    Delahay G, Duprez D. Effect of sulphur on the coking of rhodium in the steam reforming of 1-
666           methylnaphthalene. Appl Catal 1989;53:95–105. doi:10.1016/S0166-9834(00)80014-7.

667    [52]    Strohm JJ, Zheng J, Song C. Low-temperature steam reforming of jet fuel in the absence and
668           presence of sulfur over Rh and Rh-Ni catalysts for fuel cells. J Catal 2006;238:309–20.
669           doi:10.1016/j.jcat.2005.12.010.

670    [53]    Leone P, Matencio T, Garciä ME, Domigues ZR, Lanzini A, Santarelli M. Limiting Factors for a
671           Planar Solid Oxide Fuel Cell Under Different Flow and Temperature Conditions. Fuel Cells 2013:n/a-
672           n/a. doi:10.1002/fuce.201200154.

673    [54]    Rasmussen JFB, Hagen A. The effect of H2S on the performance of Ni-YSZ anodes in solid oxide
674           fuel cells. J Power Sources 2009;191:534–41. doi:10.1016/j.jpowsour.2009.02.001.

675    [55]    Rasmussen JFB, Hagen A. The Effect of H 2 S on the Performance of SOFCs using Methane
676           Containing Fuel 2010:1135–42. doi:10.1002/fuce.201000012.

677    [56]    Zha S, Cheng Z, Liu M. Sulfur Poisoning and Regeneration of Ni-Based Anodes in Solid Oxide Fuel
678           Cells. J Electrochem Soc 2007;154:B201–6. doi:10.1149/1.2404779.

679    [57]    Cheng Z, Zha S, Liu M. Influence of cell voltage and current on sulfur poisoning behavior of solid
680           oxide fuel cells. J Power Sources 2007;172:688–93. doi:10.1016/j.jpowsour.2007.07.052.

681    [58]    Aravind PV, Ouweltjes JP, Schoonman J. Diffusion Impedance on Nickel/Gadolinia-Doped Ceria
682           Anodes for Solid Oxide Fuel Cells. J Electrochem Soc 2009;156:B1417–22. doi:10.1149/1.3231490.

683    [59]    Ivey DG, Brightman E, Brandon N. Structural modifications to nickel cermet anodes in fuel cell
684           environments. J Power Sources 2010;195:6301–11. doi:10.1016/j.jpowsour.2010.04.059.

685    [60]    Arnold M, Kajolinna T. Development of on-line measurement techniques for siloxanes and other
686           trace compounds in biogas. Waste Manag 2010;30:1011–7. doi:10.1016/j.wasman.2009.11.030.

687    [61]    Arnold M. Reduction and monitoring of biogas trace compounds. 2009.

688

**<u>Highlights</u>**

- Ni catalyst stability is achieved with biogas mixture with CH4/CO2>1

- CH4/CO2=50/50 vol. % is much more harmful under steam reforming conditions both in terms of activity and stability

- The impact of trace contaminants not removed from the cleaning section from biogas are investigated on SOFCs